

Vision-Based Obstacle Avoidance for UAVs

Yoko Watanabe*, Anthony J. Calise[†] and Eric N. Johnson[‡]

Georgia Institute of Technology, Atlanta, GA, 30332

This paper describes a vision-based navigation and guidance design for UAVs for a combined mission of waypoint tracking and collision avoidance with unforeseen obstacles using a single 2-D passive vision sensor. An extended Kalman filter (EKF) is applied to estimate a relative position of obstacles from vision-based measurements. The stochastic z -test value is used to solve a correspondence problem between the measurements and the estimates that have been already obtained by then. A collision cone approach is used as a collision criteria in order to examine if there is any obstacle that is critical to the vehicle. A guidance strategy for collision avoidance is designed based on a minimum-effort guidance (MEG) method for multiple target tracking. The vision-based navigation and guidance designs suggested in this paper are integrated with realtime image processing algorithm and the entire vision-based control system are evaluated in the closed-loop 6 DoF flight simulation.

I. Introduction

Autonomous operation of Unmanned Aerial Vehicles (UAVs) has been progressively developed in recent years. In particular, vision-based navigation, guidance and control has been one of the most focused research topics for the automation of UAVs. This is because in nature, birds and insects use vision as an exclusive sensor for object detection and navigation. Furthermore, it is efficient to use a vision sensor since it is compact, light-weight and low cost. Vision-based autonomous flight of UAVs is expected to be applied for practical missions in both military and commercial fields. For some missions UAVs have to operate in congested environments that include both fixed and moving obstacles. For such missions, obstacle avoidance is an anticipated requirement. Therefore, this paper focuses on vision-based navigation and guidance system design for UAVs to detect and avoid unforeseen obstacles while executing a waypoint tracking mission.

Kumar and Ghose proposed a navigation and guidance law that achieves both waypoint tracking and collision avoidance.¹ However, this algorithm assumes range information is available from a radar. Furthermore, the flight is restricted in a 2-D plane. A method described in a paper by Kwag and Kang also assumes a radar sensor system for collision avoidance.² In this paper a 3-D state of each obstacle is estimated from 2-D vision-based information. We assume that an image processor is available which is capable of detecting multiple obstacles in each image obtained from a 2-D vision sensor. Specifically in our work, a real-time image processor based on active contours developed by Ha et al. is used.³ Since the vision-based measurement is a nonlinear function of the relative state, an Extended Kalman Filter (EKF) is applied to the navigation filter design. There is the possibility of more than one obstacle being detected in the image frame. In such a case, every obstacle in the measurement set is matched with estimated obstacle data before applying the EKF procedure. The statistical z -test value^{4,5} is introduced to perform this correspondence.

Once estimated obstacle states are obtained, a collision criterion is applied to each obstacle in order to examine if the obstacle is critical to the vehicle or not. A collision cone approach is suggested by Chakravarthy and Ghose.⁶ A collision cone is defined for each obstacle by a set of tangential lines to the obstacle's collision-safety boundary. An obstacle is considered to be critical if the relative velocity vector lies within its collision cone. Their algorithm is limited to a case in which a vehicle and obstacles stay in a 2-D plane. In this paper, the collision cone approach is extended so that it can be applied to a 3-D collision avoidance problem by considering only a 2-D plane including the relative position and velocity vectors of an obstacle with respect

*Graduate Research Assistant, Email: yoko.watanabe@ae.gatech.edu

[†]Professor, Email: anthony.calise@aerospace.gatech.edu

[‡]Lockheed Martin Assistant Professor of Avionics Integration, Email: eric.johnson@aerospace.gatech.edu

to the vehicle. If there is more than one critical obstacle, the closest is chosen as the most critical and an collision avoidance maneuver is executed with respect to only the critical obstacle.

After the most critical obstacle is identified, an aiming point is given at the intersection of the collision cone and the collision-safety boundary. In order to avoid the obstacle, the vehicle is guided towards the aiming point. Hence, the collision avoidance and waypoint tracking problem is reduced to a two-waypoints tracking problem. As a guidance strategy for collision avoidance, proportional navigation (PN)-based guidance have been suggested by Han and Bang and the present authors.^{7,8} Then, the authors developed a Minimum-Effort Guidance (MEG) design⁹ based on Asher's work which was originally developed for multiple target tracking.^{10,11} MEG-based guidance minimizes the control effort required for the vehicle to reach the waypoint via the aiming point, while the PN-based approach minimizes the effort required to reach the aiming point then to reach the waypoint in a sequential manner. Consequently MEG-based guidance can achieve the mission with less control effort compared to PN-based guidance. This is important when maneuvering in congested environments with limited maneuver capability.

The entire vision-based navigation and guidance system for obstacle avoidance has been integrated with a real-time image processor and implemented in a 6 DoF UAV flight simulation. The vehicle modeled is the YAMAHA RMax helicopter. The own-ship navigation system and a neural-network based adaptive flight controller have been previously implemented.^{12,13} It is assumed that the vehicle has a camera and its images are also simulated. The synthetic images are processed by the image processor. The algorithms are evaluated in simulations of air-to-air collision avoidance with multiple stationary obstacles.

This paper is organized as follows. SectionII formulates the vehicle motion dynamics and its guidance mission. SectionIII presents a vision-based relative navigation filter design using the z -test to address the correspondence problem. SectionIV discusses collision criteria and SectionV derives a guidance law for obstacle avoidance. The simulation results are presented in SectionVI. SectionVII includes concluding remarks.

II. Problem Formulation

Figure 1 summarizes the problem geometry. Let F_L be a local fixed frame. Let $\mathbf{X}_v, \mathbf{V}_v$ be a vehicle's position and velocity vector expressed in F_L . Let \mathbf{a} be the vehicle's acceleration input vector in F_L . Then the vehicle motion dynamics is modeled by

$$\dot{\mathbf{X}}_v = \begin{bmatrix} \dot{X}_v \\ \dot{Y}_v \\ \dot{Z}_v \end{bmatrix} = \begin{bmatrix} U_v \\ V_v \\ W_v \end{bmatrix} = \mathbf{V}_v \quad (1)$$

$$\dot{\mathbf{V}}_v = \begin{bmatrix} \dot{U}_v \\ \dot{V}_v \\ \dot{W}_v \end{bmatrix} = \begin{bmatrix} a_x \\ a_y \\ a_z \end{bmatrix} = \mathbf{a} \quad (2)$$

In this problem, $a_x = 0$ is always applied so that the vehicle maintains a constant speed in the X -direction in F_L . The vehicle is controlled by commanding a lateral acceleration a_y and a vertical acceleration a_z only. The vehicle's state is assumed to be available through the own-ship navigation filter. A camera is mounted on the vehicle and its attitude is assumed to be known in the form of a rotation matrix from the local frame F_L to the camera frame F_C , which is denoted by L_{CL} .

Let $\mathbf{X}_{wp} = [X_{wp} \ Y_{wp} \ Z_{wp}]^T$ be a given waypoint location in F_L . Then the waypoint tracking problem is achieved if

$$Y_v(t_f) = Y_{wp}, \quad Z_v(t_f) = Z_{wp} \quad (3)$$

where t_f is a time at which $X_v(t_f) = X_{wp}$ is satisfied. Let \mathbf{X}_{obs} be obstacle's position in F_L and assume $\dot{\mathbf{X}}_{obs} = \mathbf{0}$, i.e., stationary obstacles. Then the obstacle's relative motion dynamics with respect to the vehicle is written by

$$\dot{\mathbf{X}} = \dot{\mathbf{X}}_{obs} - \dot{\mathbf{X}}_v = -\mathbf{V}_v \quad (4)$$

where $\mathbf{X} = \mathbf{X}_{obs} - \mathbf{X}_v = [X \ Y \ Z]^T$ is a relative position vector in F_L . For collision avoidance, the vehicle is required to keep a minimum distance d from every obstacle. That is, a collision-safety boundary becomes a spherical surface with a radius d and a center at \mathbf{X}_{obs} . Therefore, a mission given to the vehicle is to satisfy (3) while always maintaining $\|\mathbf{X}\| \geq d$ for all obstacles. However, the obstacle's location \mathbf{X}_{obs}

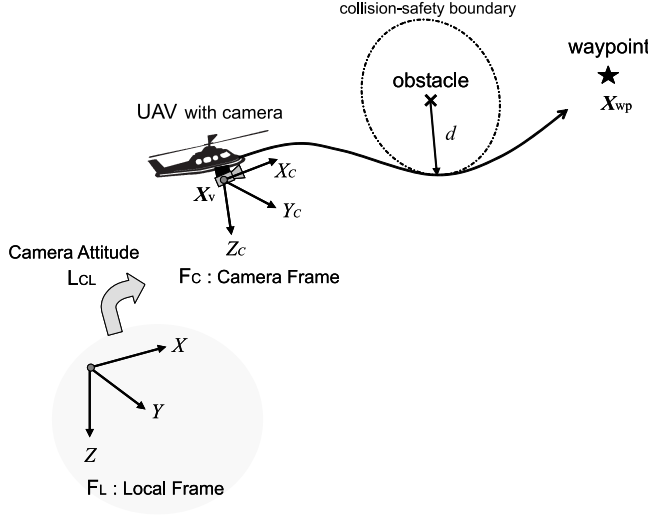


Figure 1. Problem Geometry

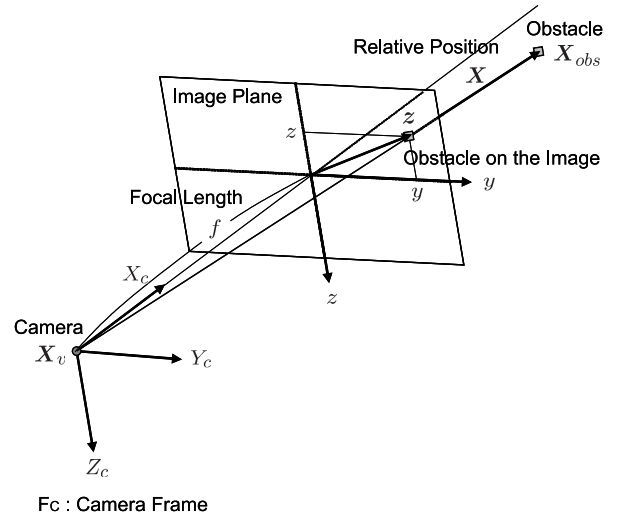


Figure 2. Pin-Hole Camera Model

is unknown to the vehicle, and so the relative position \mathbf{X} is also unknown. Hence, for obstacle avoidance, the guidance system can only use its estimate which is updated by using 2-D vision-based information from the camera.

III. Vision-Based Relative Navigation Design

A. Measurement Model

The camera frame F_C is taken so that the X_c -axis aligns with the camera's optical axis. Let $\mathbf{X}_c = L_{CL}\mathbf{X} = [X_c \ Y_c \ Z_c]^T$ be the relative position vector expressed in F_C . Assuming the pin-hole camera model shown in Figure 2, the 2-D measurement of the obstacle position in an image plane at a k -th time step is given by

$$\mathbf{z}_k = \frac{f}{X_{c_k}} \begin{bmatrix} Y_{c_k} \\ Z_{c_k} \end{bmatrix} + \boldsymbol{\nu}_k = \mathbf{h}(\mathbf{X}_{c_k}) + \boldsymbol{\nu}_k \quad (5)$$

where f is a focal length of the camera and $\boldsymbol{\nu}_k$ is a zero mean Gaussian discrete white noise process with covariance matrix $R_k = \sigma^2 I$.

B. Extended Kalman Filter

Since the measurement model (5) is nonlinear with respect to the relative state, an Extended Kalman Filter (EKF) is applied to estimate the relative position vector \mathbf{X} of each obstacle. The EKF for the process model (2,4) and the measurement model (5) is formulated as follows.^{14,15}

1. Update

The EKF update procedure is performed by using the residual between the actual measurement and the predicted measurement.

$$\hat{\mathbf{X}}_k = \hat{\mathbf{X}}_k^- + K_k(\mathbf{z}_k - \hat{\mathbf{z}}_k^-) \quad (6)$$

$$P_k = P_k^- - K_k H_k P_k^- \quad (7)$$

$$K_k = P_k^- H_k (H_k P_k^- H_k^T + R_k)^{-1} \quad (8)$$

where $\hat{\mathbf{X}}_k$ is an updated estimate of \mathbf{X} at a k -th time step and P_k is its error covariance matrix. K_k is a Kalman gain. $\hat{\mathbf{X}}_k^-$ and P_k^- are a predicted estimate and its error covariance matrix. A predicted

measurement is obtained by $\hat{\mathbf{z}}_k^- = \mathbf{h}(L_{CL_k} \hat{\mathbf{X}}_k^-)$ where L_{CL_k} is a camera attitude at the k -th time step. and a measurement matrix H_k is calculated by

$$H_k = \frac{\partial \mathbf{h}(L_{CL_k} \mathbf{X})}{\partial \mathbf{X}} \Big|_{\mathbf{X}=\hat{\mathbf{X}}_k^-} = \frac{1}{\hat{X}_{c_k}^-} \begin{bmatrix} -\frac{\hat{Y}_{c_k}^-}{\hat{X}_{c_k}^-} & 1 & 0 \\ -\frac{\hat{Z}_{c_k}^-}{\hat{X}_{c_k}^-} & 0 & 1 \end{bmatrix} L_{CL_k} = \frac{1}{\hat{X}_{c_k}^-} \begin{bmatrix} -\mathbf{h}(\hat{\mathbf{X}}_{c_k}^-) & I \end{bmatrix} L_{CL_k} \quad (9)$$

2. Prediction

The EKF prediction procedure propagates the updated estimate obtained at a current time step k to the next time step $k+1$ through the process model (2,4).

$$\hat{\mathbf{X}}_{k+1}^- = \hat{\mathbf{X}}_k - \mathbf{V}_{v_k} \Delta t_k - \frac{1}{2} \mathbf{a}_k \Delta t_k^2 \quad (10)$$

$$P_{k+1}^- = \Phi_k P_k \Phi_k^T + Q_k \quad (11)$$

where $\Delta t_k = t_{k+1} - t_k$ is a sampling time. Φ_k is a state transition matrix and which can be approximated by

$$\Phi_k \simeq I$$

for stationary obstacles when Δt_k is sufficiently small. Q_k is a covariance matrix of the process noise. The form $Q_k = \sigma_X^2 I \cdot \Delta t_k$ is used in the filter design.

C. Correspondence Problem

Since there can be multiple obstacles in the vehicle's surroundings, the image processor may detect more than one obstacle in the same image frame. Suppose that n different obstacles (denoted by $\mathbf{z}_{k_1}, \mathbf{z}_{k_2}, \dots, \mathbf{z}_{k_n}$) are detected on an image given at the k -th time step. Also suppose that the predicted estimate of the relative position of m obstacles (denoted by $\hat{\mathbf{X}}_{k_1}^-, \hat{\mathbf{X}}_{k_2}^-, \dots, \hat{\mathbf{X}}_{k_m}^-$) have been obtained by that time and stored in the database. In order to update each estimate correctly, it is very important to create a right correspondence between the measurements and the estimates before applying the EKF procedure. The statistical z -test^{4,5} is used for this purpose. In this problem, the z -test value of the correspondence between i -th measurement and j -th estimate is calculated for the residual

$$\mathbf{r}_{ij} = \mathbf{z}_{k_i} - \hat{\mathbf{z}}_{k_j}^- = \mathbf{z}_{k_i} - \mathbf{h}(L_{CL_k} \hat{\mathbf{X}}_{k_j}^-) \quad (12)$$

Then the z -test value is defined by

$$ztest_{ij} = \mathbf{r}_{ij}^T \mathbf{E}^{-1} [\mathbf{r}_{ij} \mathbf{r}_{ij}^T] \mathbf{r}_{ij} = \mathbf{r}_{ij}^T \left(H_{k_j} P_{k_j}^- H_{k_j}^T + R_k \right)^{-1} \mathbf{r}_{ij} \quad (13)$$

where H_{k_j} and P_{k_j} are the measurement matrix and the predicted error covariance matrix associated with the j -th predicted estimate. The z -test value given in (13) is inversely related to the likelihood of an event that the i -th measurement comes from the same obstacle as the j -th predicted estimate is estimating. Therefore, a small z -test value indicates a high correspondence between a chosen pair $(\mathbf{z}_{k_i}, \hat{\mathbf{X}}_{k_j}^-)$. For each measurement, the z -test value is calculated for every predicted estimate. Then the estimate which attains the least z -test value is chosen to be updated by using that measurement. In other words, \mathbf{z}_{k_i} updates the predicted estimate $\hat{\mathbf{X}}_{k_j}^-$ if

$$ztest_{ij} = \min\{ztest_{i1}, ztest_{i2}, \dots, ztest_{im}\} \quad (14)$$

is satisfied. However, when the minimum z -test value is still larger than a certain threshold value, the estimate is considered to come from a newly detected obstacle and the new estimated obstacle position $\hat{\mathbf{X}}_{k_{m+1}}$ is added to the existing estimate set. After all the correspondences are made, there may remain a predicted estimate which has not yet been updated. This happens when the corresponding obstacle lies outside of the camera's field of view or when the image processor fails to detect it. For such an estimate, only the EKF prediction procedures (10,11) are executed. The absence of a measurement corresponds to having a measurement having an infinitely large noise. When $R_k = \infty$ in (8), the Kalman gain becomes zero and no change is made in the EKF update procedure (6,7).

IV. Collision Criteria

For purposes of obstacle avoidance, each obstacle in the estimate set is examined to determine if it is critical to the vehicle using the latest updated estimate of the obstacle positions. Chakravarthy and Ghose suggested a 2-D collision cone approach to establish a collision criteria.⁶ In the collision cone approach, a collision cone is defined for each obstacle and an obstacle is considered to be critical if the relative velocity vector lies within its collision cone. This approach has been extended to 3-D in Ref.⁹ In this problem, the vehicle is required to maintain a minimum separation distance d from every obstacle. Therefore, for each obstacle, a collision-safety boundary is taken as a spherical surface with radius d and center at the obstacle position. Then a collision cone is defined by a set of tangential lines from the vehicle to the obstacle's collision safety boundary. Consider the vehicle at \mathbf{X}_{v_k} with its velocity \mathbf{V}_{v_k} at a time step k . For an obstacle located at \mathbf{X}_{obs} , let $\mathbf{X}_k = \mathbf{X}_{obs} - \mathbf{X}_{v_k}$ be the relative position of the obstacle with respect to the vehicle. Consider a 2-D plane including the relative position vector \mathbf{X}_k and the vehicle velocity vector \mathbf{V}_{v_k} . Then the collision-safety boundary appears as a circle and the collision cone is specified by two vectors (\mathbf{p}_1 , \mathbf{p}_2) which are from the vehicle position and are tangential to the boundary circle, as shown in Figure 3. \mathbf{p}_1 and \mathbf{p}_2 can be expressed as follows.

$$\mathbf{p}_i = \mathbf{X}_k + d\mathbf{u}_i, \quad i = 1, 2 \quad (15)$$

where \mathbf{u}_1 and \mathbf{u}_2 be a unit vector from the obstacle position to each of the two different points.

$$\begin{cases} \mathbf{u}_1 = -\frac{1}{\|\mathbf{X}_k\|^2} (c(\mathbf{X}_k \cdot \mathbf{V}_{v_k}) + d) \mathbf{X}_k + c\mathbf{V}_{v_k} \\ \mathbf{u}_2 = \frac{1}{\|\mathbf{X}_k\|^2} (c(\mathbf{X}_k \cdot \mathbf{V}_{v_k}) - d) \mathbf{X}_k - c\mathbf{V}_{v_k}, \quad c = \sqrt{\frac{\|\mathbf{X}_k\|^2 - d^2}{\|\mathbf{X}_k\|^2 \|\mathbf{V}_{v_k}\|^2 - (\mathbf{X}_k \cdot \mathbf{V}_{v_k})^2}} \end{cases} \quad (16)$$

The vehicle velocity vector can be written in terms of \mathbf{p}_1 and \mathbf{p}_2 .

$$\mathbf{V}_{v_k} = a\mathbf{p}_1 + b\mathbf{p}_2 \quad (17)$$

where the coefficients a and b are calculated as follows.

$$a = \frac{1}{2} \left(\frac{\mathbf{X}_k \cdot \mathbf{V}_{v_k}}{\|\mathbf{X}_k\|^2 - d^2} + \frac{1}{cd} \right), \quad b = \frac{1}{2} \left(\frac{\mathbf{X}_k \cdot \mathbf{V}_{v_k}}{\|\mathbf{X}_k\|^2 - d^2} - \frac{1}{cd} \right) \quad (18)$$

Then, the collision cone criterion is given by

$$a > 0 \quad \text{AND} \quad b > 0 \quad (19)$$

When (19) is satisfied, the vehicle is considered to be in danger of collision with the obstacle and it should take some avoiding maneuver. The aiming point \mathbf{X}_{ap} is specified to be used for collision avoidance, as shown in Figure 3.

$$\mathbf{X}_{ap} = \begin{bmatrix} X_{ap} \\ Y_{ap} \\ Z_{ap} \end{bmatrix} = \begin{cases} \mathbf{p}_1, & 0 < b \leq a \\ \mathbf{p}_2, & 0 < a < b \end{cases} \quad (20)$$

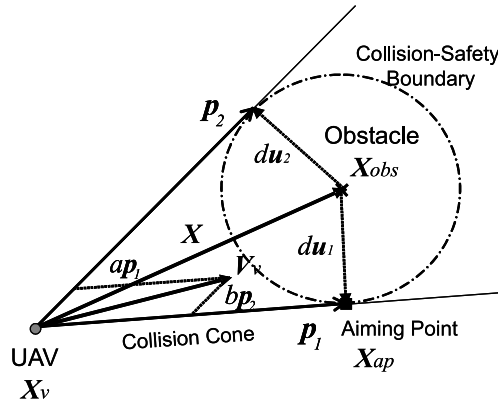


Figure 3. Collision Cone and Aiming Point

Since the vehicle has a constant speed in the X -direction, a time-to-go to the aiming point is derived as follows.

$$t_{go} = t_k + \frac{X_{ap} - X_{v_k}}{U_{v_k}} \quad (21)$$

When $(t_{go} - t_k)$ is larger than a given threshold T , there is no urgency for the vehicle to take an avoiding maneuver. Also, if it is negative or t_{go} is larger than the terminal time t_f , there is no chance of collision. Therefore, in addition to the collision cone criterion, we impose the following time-to-go criteria.

$$t_{go} - t_k < T \quad \text{AND} \quad 0 < t_{go} < t_f \quad (22)$$

An obstacle is considered to be critical only if both (19) and (22) are satisfied. If there is more than one critical obstacles, the one having the smallest time-to-go is chosen as the most critical obstacle.

V. Minimum-Effort Guidance

In this section, a guidance law is design to achieve waypoint tracking with obstacle avoidance. When there is no critical obstacle, the guidance input can be derived by solving the following minimization problem.

$$\min_{\mathbf{a}} J = \frac{1}{2} \int_{t_k}^{t_f} \mathbf{a}^T(t) \mathbf{a}(t) dt = \frac{1}{2} \int_{t_k}^{t_f} (a_y^2(t) + a_z^2(t)) dt \quad (23)$$

subject to the vehicle dynamics (1,2), with a terminal constraint (3). The terminal time t_f is given by

$$t_f = t_k + \frac{X_{wp} - X_{v_k}}{U_{v_k}} \quad (24)$$

Since the waypoint location and the vehicle's own-ship states are known, the optimal guidance can be realized as

$$\mathbf{a}_k^* = 3 \left(\frac{1}{(t_f - t_k)^2} \begin{bmatrix} 0 \\ Y_{wp} - Y_{v_k} \\ Z_{wp} - Z_{v_k} \end{bmatrix} - \frac{1}{(t_f - t_k)} \begin{bmatrix} 0 \\ V_{v_k} \\ W_{v_k} \end{bmatrix} \right) \quad (25)$$

This solution is well known as PN guidance, which is considered a simple and very effective strategy in target interception.¹⁶ When there is a critical obstacle, a corresponding aiming point \mathbf{X}_{ap} and time-to-go t_{go} are given from the collision criteria. However, since the obstacles' true positions are unknown, we can only obtain their estimated values $\hat{\mathbf{X}}_{ap}$ and \hat{t}_{go} . In order to avoid a collision with the most critical obstacle, the vehicle should fly towards the aiming point. The MEG-based guidance law^{10,11} is derived by solving the same minimization problem given in (23) with an additional interior point constraint.

$$Y_v(\hat{t}_{go}) = \hat{Y}_{ap}, \quad Z_v(\hat{t}_{go}) = \hat{Z}_{ap} \quad (26)$$

From Euler-Lagrange equations,¹⁷ this problem can be solved analytically as follows.

$$\mathbf{a}_k = \mathbf{a}_k^* + \frac{3}{3(\hat{t}_{go} - t_k) + 4(t_f - \hat{t}_{go})} \left(\frac{3}{\hat{t}_{go} - t_k} \begin{bmatrix} 0 \\ \hat{Y}_{ap} - Y_{v_k} \\ \hat{Z}_{ap} - Z_{v_k} \end{bmatrix} - \frac{2}{t_f - \hat{t}_{go}} \begin{bmatrix} 0 \\ Y_{wp} - \hat{Y}_{ap} \\ Z_{wp} - \hat{Z}_{ap} \end{bmatrix} - \begin{bmatrix} 0 \\ V_{v_k} \\ W_{v_k} \end{bmatrix} \right) \quad (27)$$

where \mathbf{a}_k^* is the PN guidance input given in (25).⁹

VI. 6 DoF Image-in-the-Loop Simulation

A. UAV Flight Simulation

The vision-based relative navigation filter designed in Section III, the collision criteria defined in Section IV and the minimum-effort guidance law derived in Section V have been implemented in a 6 DoF UAV flight simulation. A vehicle modeled in the simulation is the unmanned helicopter GTMax (Figure 4), which is based on the YAMAHA RMax industrial helicopter. The GTMax has a rotor diameter of 10.2 (ft) and a weight of approximately 157 (lbs). The basic flight controller, own-ship navigation and guidance system of the vehicle have already been implemented.¹² The controller is an adaptive neural network flight controller and it determines actuator inputs based on the navigation system output and position/velocity/acceleration commands.¹³ In addition, the vehicle has a camera and its image is also simulated. The synthetic images are processed and result in a detected obstacle's image coordinate in pixels. The image processor has been developed for real-time target tracking by using an active contour method.^{3,18} Figure 5 is a display of the flight simulation in an obstacle avoidance configuration. Red spheres are obstacles which the vehicle needs to avoid. The window on the left is a map view from the top and the yellow line is the vehicle trajectory. The window at the top right shows a synthetic camera image in the simulation. The image processor outputs are represented by small green crosses in this window. The image processor is detecting the center positions of two obstacles in this picture. The right bottom window displays a chase view from behind of the vehicle. The estimated obstacle positions are indicated in the map view and the chase view windows.

B. Simulation Settings

Before starting a mission, the vehicle is commanded to fly upward 400 (ft) and then forward 200 (ft) to reach a starting point $\mathbf{X}_0 = [200 \ 0 \ -400]^T$ (ft) by using the basic guidance system. At the same time, the vehicle is commanded to pass through the point \mathbf{X}_0 with its velocity $\mathbf{V}_0 = [50 \ 0 \ 0]^T$ (ft/sec). As soon as the vehicle passes the starting point, the entire system for the vision-based obstacle avoidance is turned on and the guidance system is switched to the one described in Section V. The vehicle is required to fly 1600 (ft) forward from the starting point, which means that a waypoint is given at $\mathbf{X}_{wp} = [1800 \ 0 \ -400]^T$ (ft). On the way to the waypoint, there exist two unforeseen stationary obstacles at $\mathbf{X}_{obs_1} = [600 \ 50 \ -420]^T$ (ft) and $\mathbf{X}_{obs_2} = [1200 \ 0 \ -400]^T$ (ft). Both obstacles are given as a sphere with radius 20 (ft). To avoid a collision, the vehicle needs to maintain at least a minimum separation distance $d = 100$ (ft) from both of the obstacles for entire flight path. After reaching the waypoint, the guidance system is switched back to the basic one and it guides the vehicle to reach and stop at the terminal point $\mathbf{X}_f = [2000 \ 0 \ -400]^T$ (ft).

For the navigation filter design, $\sigma = 0.1$ and $\sigma_X = 0.1$ were used for the measurement noise covariance matrix R_k and for the process noise covariance matrix Q_k , respectively. The EKF is initialized by using the first measurement \mathbf{z}_0 obtained for each obstacle. It is assumed that we have some knowledge about range r_0 (only for the initialization). Then the initial estimate of a relative position and its error covariance matrix



Figure 4. GTMax

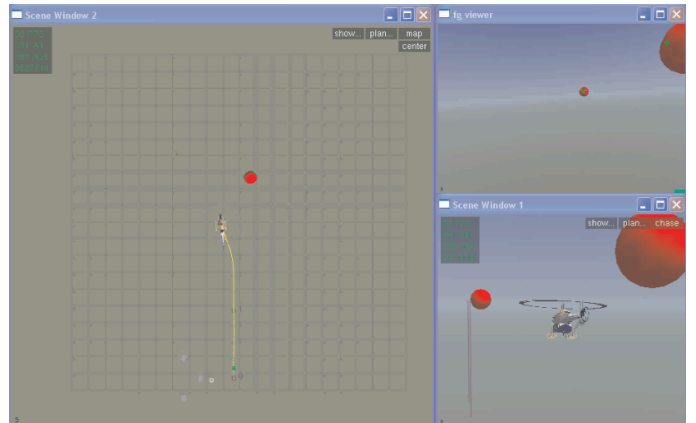


Figure 5. Simulation Interface

are set as

$$\hat{\mathbf{X}}_0 = r_0 \begin{bmatrix} 1 \\ \mathbf{z}_0 \end{bmatrix}, \quad P_0 = L_{LC_0} \begin{bmatrix} \sigma_r^2 & 0 \\ \mathbf{0} & r_0 R_k \end{bmatrix} L_{LC_0}^T \quad (28)$$

In the simulation, $r_0 = 300$ (ft) was used for the first obstacle and $r_0 = 800$ (ft) was used for the second one, and $\sigma_r = 50$ (ft) was used for the both. If the image processor detects both obstacles immediately after starting the mission, the first and second obstacles are 400 (ft) and 1000 (ft) ahead of the vehicle at that time. Therefore, initially, a range to the first obstacle is underestimated by 100 (ft) and that to the second one is underestimated by 200 (ft). For the correspondence problem, $z_{test_{max}} = 3$ was set as a threshold value. By looking at the z -table,⁵ this threshold value implies that a hypothesis of the correspondence is rejected when its likelihood is less than 9.364 %. In the collision criteria, a threshold value for the time-to-go used in the simulation was $T = 4$ (sec). Since the vehicle maintains approximately 50 (ft/sec) speed in the X -direction, $T = 4$ (sec) means that an obstacle is not considered to be critical if it has a range more than double of the minimum separation d from the vehicle.

C. Results

1. Image Processing

Figure 6 includes plots of a number of obstacles which are detected by the image processor, and their image coordinates \mathbf{z} . In this simulation, the vehicle reached at the starting point \mathbf{X}_0 at $t_0 = 69.9$ (sec), passed by the first obstacle \mathbf{X}_{obs_1} (Obstacle1) at $t_1 = 78.1$ (sec) and the second obstacle \mathbf{X}_{obs_2} (Obstacle1) at $t_2 = 91.5$ (sec), and finally reached the waypoint \mathbf{X}_{wp} at $t_f = 106.1$ (sec). From Figure 6, until $t = 74.5$ (sec), the image processor detected only Obstacle1. After that, Obstacle1 went out of the camera's field of view, and the image processor started to detect Obstacle2 until 87.5 (sec). So the image processor did not capture both two obstacles in the same image frame in this example. In Figure 6, the image coordinates of each obstacle's position detected by the image processor are compared with those calculated by using true states of the vehicle and the obstacles. They are perfectly matched at the beginning, but the measurement error becomes larger as the vehicle (or camera) comes closer to the obstacle. An average processing time was $\Delta t = 0.1213$ (sec).

2. Estimation

Figure 7 shows z -test results for a correspondence between measurements and estimates. At initial time t_0 , an estimated obstacle data $\hat{\mathbf{X}}_1$ which corresponds to Obstacle1 was created based on the first measurement \mathbf{z}_0 . After that, the z -test value is calculated to check a correspondence between the measurement \mathbf{z} and the updated estimate $\hat{\mathbf{X}}_1$ at each time step. At $t = 74.5$ (sec), the z -test value became larger than its threshold $z_{test_{max}} = 3$ and a new estimated obstacle data $\hat{\mathbf{X}}_2$ which corresponds to Obstacle2 was created. From that point, the z -test values are calculated to check a correspondence between the measurement \mathbf{z} and two estimates $\hat{\mathbf{X}}_1$ and $\hat{\mathbf{X}}_2$. From Figure 7, it can be seen that the z -test value for $\hat{\mathbf{X}}_1$ is much larger than that

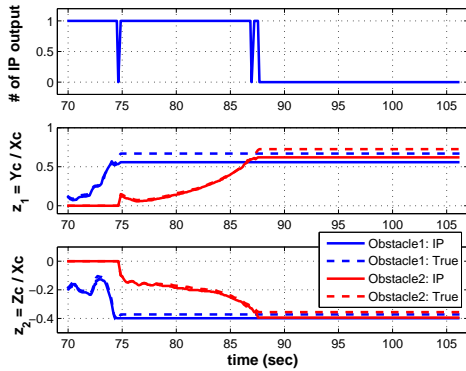


Figure 6. Image Processor Outputs

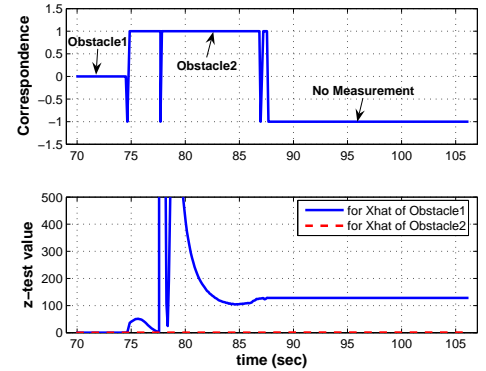


Figure 7. Correspondence Results and z -test Values

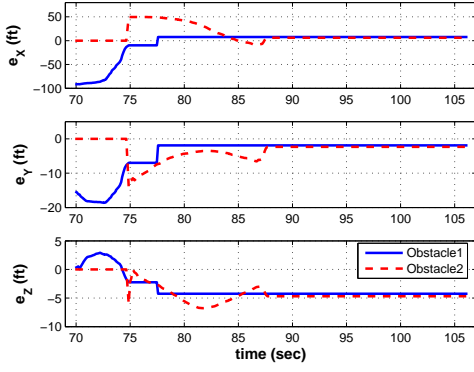


Figure 8. Position Estimation Errors

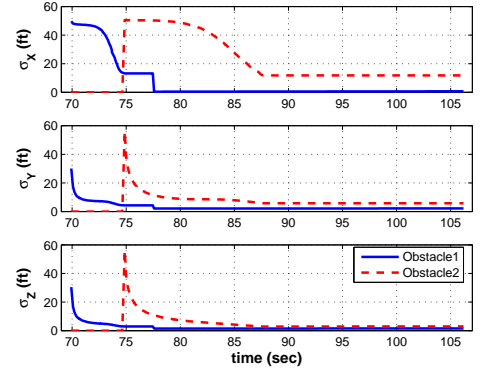


Figure 9. Standard Deviation of Errors

for $\hat{\mathbf{X}}_2$ after $t = 74.5$ (sec) and the measurement was correctly assigned to the estimated obstacle data of Obstacle2. The z -test algorithm worked well for the correspondence problem.

Figures 8 and 9 present the position estimation error and its standard deviation for each obstacle. When the estimate is initialized for each obstacle, there is a very large range estimation error e_x (ft). 100 (ft) underestimated for Obstacle1 and 50 (ft) overestimated for Obstacle2. Those estimation errors are reduced to less than 10 (ft) through the EKF updates by using the vision-based information. Even though there remains a small bias in the lateral position estimates (which is due to a bias in the measurement error), vision-based estimation performance is sufficiently accurate to be used in the collision criteria.

3. Guidance

Figure 10 shows the vehicle trajectory with positions of the starting point, the waypoint and the two obstacles. Figure 11 plots a distance from each obstacle. From those results, we can see that the suggested guidance law successfully made the vehicle reach a given waypoint while not violating the minimum separation distance $d = 100$ (ft) from the two obstacles. Figure 12, 13 and 14 are time profiles of the vehicle's position, velocity and acceleration. Figure 12 shows that the vehicle's avoiding maneuver is three dimensional. In Figure 14, the actual vehicle acceleration is compared with the commanded acceleration which is determined by the minimum-effort guidance (27). The lateral acceleration command was very large around $t = 78$ (sec). This is because the denominator $(\hat{t}_{go} - t_k)$ in (27) went close to zero. Figure 15 shows a critical obstacle flag, which is 1 when an obstacle is critical and 0 when it is not, for each obstacle. This result verified that the collision criteria established in SectionIV worked appropriately.

VII. Conclusion

This paper summarizes the design of a vision-based relative navigation and guidance system for a UAV to achieve 3-D waypoint tracking with vision-based obstacle avoidance. All the algorithms developed in this paper have been integrated with the real-time image processor and evaluated in a 6 DoF UAV flight simulation. A good performance of the entire system, which includes the image processor, the EKF-based navigation filter using the z -test to solve the correspondence problem, the collision criteria and the MEG-based guidance law, has been verified in a very realistic simulation with exactly the same configuration as an actual autonomous flight system. The next step of this work is to test the algorithms in an actual flight. Also as future work, we would like to extend the algorithm so that it can be applied to maneuvering obstacles. An adaptive estimator can be applied to estimate a relative state of moving obstacles.¹⁹

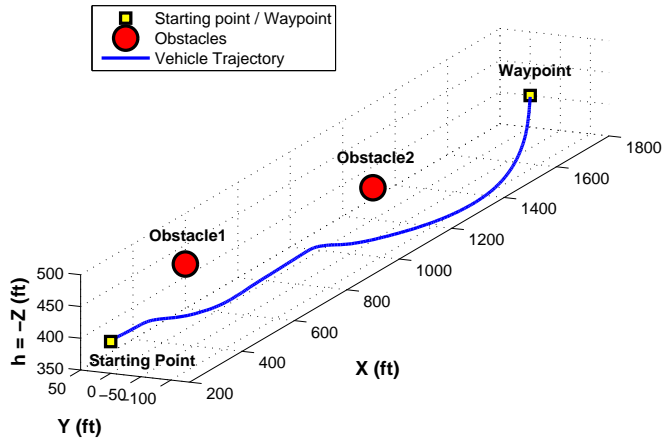


Figure 10. Vehicle Trajectory

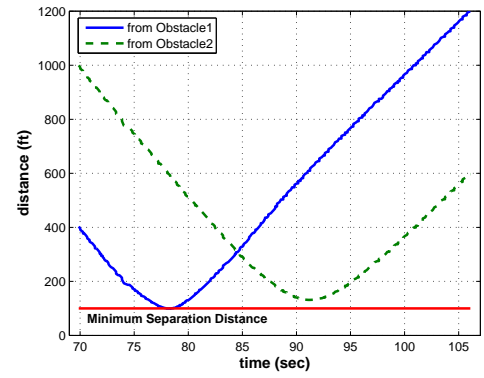


Figure 11. Distance from Obstacles

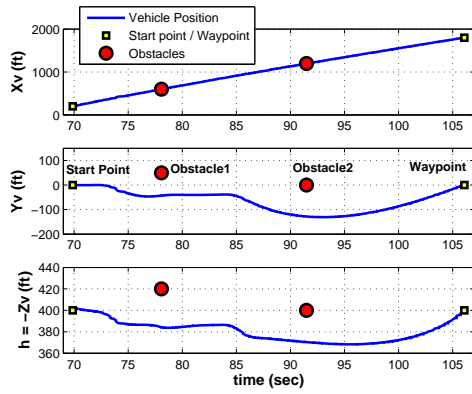


Figure 12. Vehicle Position

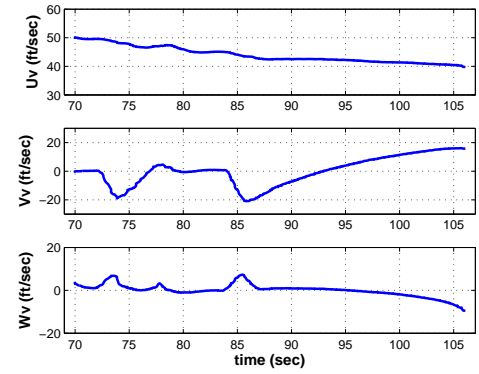


Figure 13. Vehicle Velocity

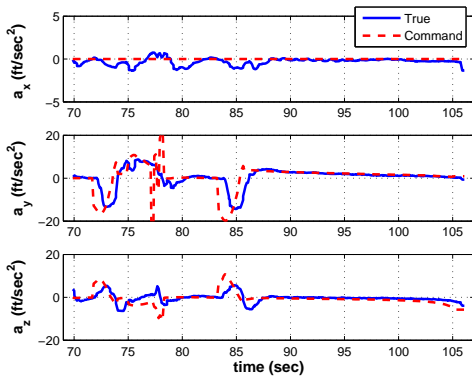


Figure 14. Vehicle Acceleration (True and Command)

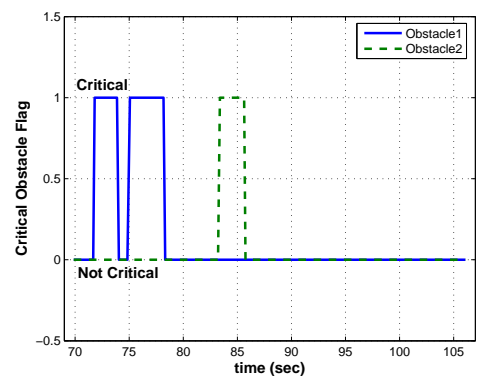


Figure 15. Critical Obstacle

VIII. Acknowledgement

This work is supported in part by AFOSR MURI, #F49620-03-1-0401: Active Vision Control Systems for Complex Adversarial 3-D Environments. We also acknowledge the contributions of Dr.Allen Tannenbaum and Jin-cheol Ha who developed the image processing algorithm, and of Nimrod Rooz who set up the simulation codes for a vision-based obstacle avoidance configuration.

References

- ¹B.A.Kumar and D.Ghose. "Radar-Assisted Collision Avoidance/Guidance Strategy for Planar Flight" IEEE Transactions on Aerospace and Electronic Systems. Vol.37, No.1. January 2001.
- ²Y.K.Kwag and J.W.Kang. "Obstacle Awareness and Collision Avoidance Radar Sensor System for Low-Altitude Flying Smart UAV" Digital Avionics Systems Conference. October 2004.
- ³J.Ha, C.Alvino, G.Prior, M.Niethammer, E.N.Johnson and A.Tannenbaum. "Active Contours and Optical Flow for Automatic Tracking of Flying Vehicles" American Control Conference. 2004.
- ⁴A.J.Hayter. "Probability and Statistics" Duxbury. 2004.
- ⁵W.H.Hines, D.C.Montgomery, D.M.Goldsman and C.M.Borror. "Probability and Statistics in Engineering" John Wiley&Sons. 2003.
- ⁶A.Chakravarthy and D.Ghose. "Obstacle Avoidance in a Dynamic Environment: A Collision Cone Approach" IEEE Transactions on Systems, Man and Cybernetics-Part A: Systems and Humans. Vol.28, No.5. 1998.
- ⁷S.C.Han and H.Bang. "Proportional Navigation-Based Optimal Collision Avoidance for UAVs" 2nd International Conference on Autonomous Robots and Agents. 2004.
- ⁸Y.Watanabe, V.K.Madyastha, E.N.Johnson and A.J.Calise. "Vision-Based Approaches to UAV Formation Flight and Obstacle Avoidance" Second International Symposium on Innovative Aerial/Space Flyer Systems. December 2005.
- ⁹Y.Watanabe, A.J.Calise, E.N.Johnson and J.H.Evers. "Minimum-Effort Guidance for Vision-Based Collision Avoidance" AIAA Atmospheric Flight Mechanics Conference. August 2006.
- ¹⁰J.Z.Ben-Asher. "Minimum-Effort Interception of Multiple Targets" AIAA Journal of Guidance, Control, and Dynamics. Vol.16, No.3. 1993.
- ¹¹J.Z.Ben-Asher and I.Yaesh. "Advances in Missile Guidance Theory" AIAA. 1998.
- ¹²E.N.Johnson and D.P.Shcraige. "The Georgia Tech Unmanned Aerial Research Vehicle: GTMax" AIAA Guidance, Navigation and Control Conference. August 2003.
- ¹³E.N.Johnson and S.K.Kannan. "Adaptive Flight Controller for an Autonomous Unmanned Helicopter" AIAA Guidance, Navigation and Control Conference. August 2002.
- ¹⁴R.G.Brown and P.Y.C.Hwang. "Introduction to Random Signals and Applied Kalman Filtering" John Wiley&Sons. 1997.
- ¹⁵P.Zarchan and H.Musoff. "Fundamentals of Kalman Filtering: A Practical Approach" AIAA. 2005.
- ¹⁶P.Zarchan. "Tactical and Strategic Missile Guidance" AIAA. 1994.
- ¹⁷A.E.Bryson and Y.Ho. "Applied Optimal Control: Optimization, Estimation, and Control" Taylor & Francis. 1975.
- ¹⁸E.N.Johnson, A.J.Calise, Y.Watanabe, J.Ha and J.C.Neidhoefer. "Real-Time Vision-Based Relative Aircraft Navigation" AIAA Journal of Aerospace Computing, Information, and Communication. vol.4, no.4. 2007.
- ¹⁹A.J.Calise, E.N.Johnson, R.Sattigeri, Y.Watanabe and V.K.Madyastha. "Estimation and Guidance Strategies for Vision-Based Target Tracking" American Control Conference. June 2005.